Frontiers in Bioscience Landmark

*Front. Biosci. (Landmark Ed)* **2025**; 30(8): 42716
https://doi.org/10.31083/FBL42716

*Original Research*

# Changes in Pre- and Post-Treatment Gut Microbiota and Metabolites in Neonates With Hyperbilirubinemia

Liyi Mo[1,†], Yanwen Luo[1,†], Yan Liu[2], Qinqin Chen[3], Minxiu Ye[3], Dongzi Lin[1,*], Cheng Xu[1,*]

[1]Department of Clinical Laboratory Medicine, The Fourth People's Hospital of Nanhai District of Foshan City, 528211 Foshan, Guangdong, China
[2]Department of Biochemistry and Molecular Biology, School of Basic Medicine, Guangdong Medical University, 524023 Zhanjiang, Guangdong, China
[3]Neonatology Department, The Fourth People's Hospital of Nanhai District of Foshan City, 528211 Foshan, Guangdong, China
*Correspondence: dongzi_001@163.com (Dongzi Lin); xucheng2190@163.com (Cheng Xu)
[†]These authors contributed equally.
Academic Editor: Amedeo Amedei
Submitted: 28 May 2025 Revised: 12 August 2025 Accepted: 18 August 2025 Published: 30 August 2025

**Abstract**

**Background**: Neonatal jaundice affects up to 60% of newborns, with pathological cases frequently associated with impaired bilirubin metabolism and gut microbiota dysbiosis. Although evidence implicates gut microbiota in bilirubin metabolism, the precise mechanisms remain incompletely characterized. This study investigated treatment-associated changes in gut microbiota composition, fecal metabolites, and liver function in neonates with hyperbilirubinemia. **Methods**: A total of forty-two neonates diagnosed with hyperbilirubinemia were recruited. Fecal samples were collected pre- and post-treatment. Gut microbiota composition was analyzed via 16S rRNA gene sequencing, while fecal metabolites were profiled using untargeted metabolomics. Liver function parameters, including serum bilirubin levels, were measured. Statistical analyses encompassed alpha/beta diversity assessments, Spearman correlation, and Kyoto Encyclopedia of Genes and Genomes (KEGG) pathway enrichment. **Results**: Post-treatment gut microbial diversity decreased significantly, marked by increased abundance of *Streptococcus thermophilus* and *Rothia* and reduced levels of *Pseudomonas* and *Staphylococcus*. Key altered metabolites included 9,11-methane-epoxy PGF1$\alpha$, prostaglandin E2 isopropyl ester, and 7-methylthioheptyl glucosinolate. Notably, *Streptococcus thermophilus* abundance inversely correlated with 7-methylthioheptyl glucosinolate but positively correlated with 9,11-methane-epoxy PGF1$\alpha$ and prostaglandin E2 isopropyl ester. Total bilirubin levels decreased significantly post-treatment, alongside improvements in other liver function markers. **Conclusions**: This study demonstrates significant treatment-associated shifts in gut microbiota and metabolites in hyperbilirubinemic neonates, suggesting microbial dysbiosis may contribute to altered bilirubin metabolism. These findings highlight the potential of early microbiome-targeted interventions for managing neonatal jaundice and identify candidate therapeutic targets and biomarkers.

**Keywords:** newborn; hyperbilirubinemia; gastrointestinal microbiome; metabolism; Rothia

## 1. Introduction

Neonatal hyperbilirubinemia, characterized primarily by jaundice, is a common condition affecting newborns. Up to 60% of full-term and 80% of preterm infants exhibit jaundice during the early postnatal period [1,2]. While most cases represent transient physiological jaundice, pathological hyperbilirubinemia can arise from conditions such as perinatal infection, isoimmune hemolysis, breast milk jaundice, and glucose-6-phosphate dehydrogenase deficiency [3]. Pathological hyperbilirubinemia poses significant neurotoxic risk; unconjugated bilirubin can cross the blood-brain barrier, potentially causing bilirubin encephalopathy and permanent neurological damage if untreated [3]. The etiology involves multiple factors, including physiological immaturity, isoimmune mechanisms, genetic variations, and environmental influences [4,5]. Notably, emerging evidence implicates gut microbiota dysbiosis as a key environmental factor associated with neonatal hyperbilirubinemia [6,7].

Both animal and clinical studies demonstrate that the gut microbiota plays a critical role in bilirubin metabolism, particularly in mediating the deconjugation of bilirubin glucuronides. Conjugated bilirubin is excreted via bile into the intestine [8], where specific gut bacteria, including *Clostridium* species (*C. perfringens*, *C. difficile*) and *Bacteroides fragilis*, catalyze its deconjugation. This process increases intestinal unconjugated bilirubin levels, promoting its reabsorption and enhancing enterohepatic circulation [9]. On the other hand, the absence of gut microbiota leads to reduced production of short-chain fatty acids (SCFA), thereby increasing the permeability of the blood-brain barrier. This allows free bilirubin to enter the central nervous system. Within neurons, excessive bilirubin triggers oxidative stress and mitochondrial alterations, ultimately resulting in neuronal apoptosis and the development of neonatal bilirubin encephalopathy. However, to date, the detailed pathways through which gut microbiota influences bilirubin metabolism and induces oxidative stress remain poorly understood [10].

Given the established link between neonatal hyperbilirubinemia and gut microbiota dysbiosis, this study employed high-throughput 16S rRNA gene sequencing to profile the abundance, composition, and diversity of the gut microbiota in hyperbilirubinemic neonates before and after treatment. Complementary untargeted metabolomic analysis was used to investigate potential mechanisms by which the gut microbiota influences hyperbilirubinemia. Our objectives were to characterize treatment-associated changes in the neonatal gut microbiome and identify associated bacterial metabolites, thereby identifying potential therapeutic targets and biomarkers for precise management of neonatal hyperbilirubinemia.

## 2. Materials and Methods

### *2.1 Subjects and Sample Collection*

Study Population and Ethics: This prospective study enrolled 42 neonates diagnosed with hyperbilirubinemia admitted to the Fourth People's Hospital of Nanhai District (Guangdong, Foshan) between February and April 2023. The study protocol was approved by the ethics committee of The Fourth People's Hospital of Nanhai District of Foshan City (Approval No.: KKNL-2023-32), and written informed consent was obtained from all parents or guardians. The study was carried out in accordance with the guidelines of the Declaration of Helsinki.

Inclusion Criteria: Neonates met all the following criteria. (1) Maternal Factors: Mother aged 20–40 years without pregnancy complications (e.g., hypertensive disorders, nephropathy, anemia, or diabetes). (2) Neonatal Factors: Vaginal delivery, absence of birth trauma or asphyxia, normal Apgar scores, birth weight 2500–4000 g, gestational age $\geq$37 weeks, postnatal age 3–30 days at enrollment, either sex. (3) Hyperbilirubinemia: Jaundice onset 3–5 days postnatally, serum total bilirubin exceeding the 95th percentile on the Bhutani curve, predominantly unconjugated hyperbilirubinemia. (4) Feeding/Medication: Breastfed within 30 minutes of birth, exclusively breastfed, no history of antibiotic or probiotic administration. Exclusion Criteria: Neonates were excluded for low birth weight ($<$2500 g), infections of other organs/tissues, immune system disorders, conditions affecting intestinal metabolism, or significant maternal illness during pregnancy.

Sample Collection and Processing: (1) Fecal Samples: Fresh fecal samples were collected from each neonate on day 1 (pre-treatment) and day 3 (post-treatment) of admission using specialized tubes containing metabolite preservation solution and microbial DNA stabilization buffer. Samples were immediately frozen at –80 °C until analysis. The specific products used for preserving fecal microbiome and metabolites in this study were the Fecal Microbiome Genome Preservation Kit (LS-R-P-007, Longsee, Guangzhou, China) and the Fecal Microbiota Metabolite Protective Solution Kit (LS-R-P-020, Longsee, Guangzhou, China). (2) Blood Samples: Venous blood was drawn concurrently with fecal sampling for routine blood tests, measurement of serum total bilirubin (TBIL) and direct bilirubin (DBIL), and quantification of C-reactive protein (CRP).

Laboratory Analyses: (1) Gut Microbiota: Microbial DNA was extracted from fecal samples, and the V3–V4 region of the bacterial 16S rRNA gene was amplified and sequenced (Illumina platform) to assess composition, diversity, and abundance. (2) Fecal Metabolomics: Untargeted metabolomic profiling of fecal samples was performed using liquid chromatography-mass spectrometry system (LC-MS/MS). (3) Blood Parameters: TBIL, DBIL, and CRP levels were measured using standard clinical laboratory methods.

### *2.2 16S rRNA Gene Sequencing*

DNA Extraction and 16S rRNA Gene Sequencing: Fecal microbial DNA was extracted using the Trace Bacterial Community DNA Extraction Kit (Magnetic Soil and Stool DNA Kit) (Tiangen Biotech, Beijing, China) according to the manufacturer's protocol. The hypervariable V3-V4 region of the bacterial 16S rRNA gene was amplified via PCR using primers containing Illumina adapter sequences: 338F (5′-ACTCCTACGGGAGGCAGCA-3′) and 806R (5′-GGACTACHVGGGTWTCTAAT-3′). Sequencing libraries were constructed from the amplified products and paired-end sequenced (2 $\times$ 250 bp) on an Illumina MiSeq-PE250 platform (San Diego, CA, USA).

Bioinformatic Processing: Raw sequencing reads were demultiplexed and assigned to samples using custom Perl and Bash scripts. Paired-end reads were merged using FLASH (v1.2.11) (https://ccb.jhu.edu/software/FLASH/). Sequence quality control, including adapter removal and quality trimming (Q20), was performed using Trimmomatic (v0.39). Chimeric sequences were identified and removed using the UCHIME algorithm within USEARCH (v11.0.667). High-quality, non-chimeric sequences were clustered into operational taxonomic units (OTUs) at 97% sequence similarity using the UPARSE algorithm in USEARCH. The most abundant sequence within each OTU was designated as the representative sequence. Taxonomic classification was assigned against the SILVA database (release 138) using a confidence threshold of 0.8.

Microbiome Analysis: Processed OTU data were analyzed for alpha diversity (Shannon, Simpson, Chao1, Observed Species indices) and beta diversity (Bray-Curtis dissimilarity, weighted/unweighted UniFrac distances). Principal Coordinates Analysis (PCoA) based on beta diversity metrics was performed. Linear discriminant analysis Effect Size (LEfSe) was used to identify differentially abundant taxa between groups. Putative functional profiles of the microbiota were predicted from the 16S data using PICRUSt2 and mapped to Kyoto Encyclopedia of Genes and Genomes (KEGG) pathways.

*2.3 Untargeted Metabolomics Analysis*

Sample Preparation: A total of 84 frozen fecal samples (100 µL each), collected from 42 neonates pre- and post-treatment, were subjected to untargeted metabolomic analysis. Each sample was mixed with 10 µL of internal standard (L-2-chlorophenylalanine, 0.3 mg/mL in methanol) and 300 µL of ice-cold extraction solvent (methanol:acetonitrile, 2:1, v/v). Ultrasound-assisted extraction was performed in an ice-water bath. Following centrifugation, 200 µL of the supernatant was transferred for LC-MS analysis.

Metabolomic analysis via LC-MS: The liquid chromatography-mass spectrometry (LC-MS) system (1290 Infinity II UHPLC/6545 Q-TOF) from Agilent Technologies Inc (Santa Clara, CA, USA). An ACE Excel2C-18PFP column (100 × 2.1 mm, 2 µm; Aberdeen, Scotland) equipped with a C18 guard column was employed. Mobile phase A consisted of water containing 0.1% formic acid, while mobile phase B was acetonitrile with 0.1% formic acid. The gradient program was as follows: 2% B (0–1 min), increased to 98% B over 9 minutes (1–10 min), held at 98% B for 2 minutes (10–12 min), decreased to 2% B over 0.5 minutes (12–12.5 min), and re-equilibrated at 2% B for 3 minutes (12.5–15.5 min). The injection volume was 2 µL, the column temperature was maintained at 35 °C, and all samples were injected in duplicate [11].

LC-MS Data Acquisition and Preprocessing: Raw data files (.abf) were converted using AbfConverter. Peak detection, alignment, and feature processing were performed using MS-DIAL software (version 4.90, RIKEN, Saitama, Japan). Compound identification was achieved by matching primary and secondary mass spectra against the MASSBANK and METLIN databases.

Quality Control and Data Filtering: Features were removed if they were (1) Detected in $<$50% of quality control (QC) samples. (2) Present in $<$50% of samples within any experimental group. For features representing the same compound, only the peak with highest identification confidence was retained; others were excluded. All retained features underwent preliminary statistical analysis. Coefficient of variation (CV) was calculated for each feature across QC samples. Features with CV $>$30% were discarded. Compound identification and relative quantification required detection in at least one sample with peak area $\geq$5-fold higher than blank controls.

Data Normalization and Statistical Analysis: Stable features were normalized using the MetaboAnalystR package (v4.2.0) (https://www.metaboanalyst.ca/). Statistical analyses included univariate analysis (two-group comparisons: Student's *t*-test (fold change calculation), or multi-group comparisons: Kruskal-Wallis H test) and multivariate analysis (Principal Component Analysis (PCA) using prcomp (R), Partial Least Squares-Discriminant Analysis (PLS-DA) using MetaboAnalystR (VIP score extraction)).

Differential Metabolite Identification: Metabolites were considered differentially abundant based on two-group comparison (VIP $>$1, $p < 0.05$, and $|\log_2$ (fold change)$| \geq 1$ (equivalent to FC $\geq$2 or $\leq$0.5)) or multi-group comparison (VIP $>$1 and $p < 0.05$).

*2.4 Statistical Analysis*

Statistical analyses were performed using SPSS (version 22.0; IBM Corp., Armonk, NY, USA) and R (version 3.1.0; R Foundation for Statistical Computing, Vienna, Austria). Clinical characteristics of neonates were analyzed using appropriate descriptive and inferential statistics.

Differences in microbiome profiles and LC-MS-derived metabolite levels between groups were assessed using either Student's *t*-test (for normally distributed variables) or the Mann-Whitney U test (for non-normally distributed variables) in R. Normality was evaluated using the Shapiro-Wilk test.

Spearman rank correlation analysis was conducted using GraphPad Prism (version 7.00; GraphPad Software, Inc., San Diego, CA, USA) to examine associations between gut microbiota composition and fecal metabolite profiles.

## 3. Results

*3.1 Clinical Characteristics of Neonates*

All 42 hyperbilirubinemic neonates were admitted to the Neonatal Department of the Fourth People's Hospital of Nanhai District, Foshan City, between February and April 2023 (see **Supplementary Material_Clinical information of the cases**). At treatment initiation (day 1), the mean serum total bilirubin (T-BIL) level was 340.5 µmol/L (corrected unit). By post-treatment day 3, T-BIL significantly decreased to 305.0 µmol/L. Comparative analysis of liver function and inflammatory markers pre- versus post-treatment revealed statistically significant reductions (all $p < 0.001$) in: Albumin (ALB), Aspartate aminotransferase (AST), Total bilirubin (T-BIL), Total protein (TP), Adenosine deaminase (ADA), C-reactive protein (CRP) (Data presented in Table 1: Clinical characteristics of the study cohort).

*3.2 Fecal Alpha and Beta Diversity in Pretherapy and Post-Treatment Neonates*

Analysis of gut microbiota structure in neonates with hyperbilirubinemia via 16S rRNA sequencing revealed *Firmicutes*, *Proteobacteria*, *Actinobacteria*, *Bacteroidetes*, and *Cyanobacteria* as the dominant phyla (Fig. 1A), with *Streptococcus*, *Bifidobacterium*, *Pseudomonas*, *Rothia*, and *Staphylococcus* predominating at the genus level (Fig. 1B). Following treatment, the relative abundance of *Firmicutes* significantly increased, while that of *Cyanobacteria* significantly decreased. At the genus level, significant increases were observed in *Streptococcus* ($p = 0.001$) and *Rothia* ($p = 0.006$), whereas *Pseudomonas* ($p = 0.014$) and *Staphylococcus* ($p = 0.022$) significantly decreased (Fig. 1C,D).

**Table 1. Clinical characteristics of the study cohort.**

| Feature | Pre (n = 42) | Post (n = 42) | *p* value |
|---|---|---|---|
| ALB (g/L) | 38.1 (32.7–43.1) | 34.2 (30.3–38.4) | <0.001 |
| ALT (U/L) | 12.4 (4.2–26.0) | 12.1 (2.0–25.5) | 0.835 |
| AST (U/L) | 40.7 (19–101) | 27.6 (16–47.7) | <0.001 |
| D-BILI (mmol/L) | 14.7 (9.3–30.2) | 14.5 (8.2–21.5) | 0.893 |
| T-BILI (mmol/L) | 312.4 (202.7–456.8) | 120.7 (65.3–227.1) | <0.001 |
| TP (g/L) | 55.3 (46.6–65.4) | 51.4 (45.2–61.9) | 0.001 |
| ALP (U/L) | 211.9 (108.6–428) | 237.4 (136.4–509) | 0.184 |
| GGT (U/L) | 150.8 (67–345) | 149.3 (62–325) | 0.935 |
| ADA (U/L) | 2.2 (0–6) | 4.3 (2–8) | <0.001 |
| TBA (mmol/L) | 18 (4.9–70.3) | 24.6 (6.1–118.1) | 0.200 |
| CRP (mg/L) | 2.1 (0–11.77) | 0.55 (0–3.92) | <0.001 |

ALB, Albumin; ALT, Alanine transaminase; AST, Aspartate aminotransferase; D-BILI, direct bilirubin; T-BILI, Total bilirubin; TP, Total protein; ALP, Alkaline phosphatase; GGT, Gamma-glutamyl transpeptidase; ADA, Adenosine deaminase; TBA, Total bile acid; CRP, C-reactive protein.

Post-treatment also significantly reduced the alpha diversity of the gut microbiota, with significant differences (all $p < 0.05$) in the Chao1, Shannon, and Simpson indices (Fig. 1E). Principal Component Analysis (PCA) of beta diversity indicated partial separation between pre- and post-treatment samples, with a statistically significant difference ($p = 0.016$; Fig. 1F).

Further LEfSe analysis (LDA threshold $\geq$3.5) identified six significantly upregulated and 28 significantly downregulated bacterial taxa post-treatment (Fig. 2A). We then investigated the correlation between these differentially abundant genera and liver function markers, including C-reactive protein (CRP), before and after treatment. Given bilirubin's role as a key indicator of neonatal hyperbilirubinemia, we specifically analyzed associations between gut microbiota and total bilirubin levels. *Staphylococcus* and *Pseudomonas* exhibited positive correlations with bilirubin levels, suggesting their increase may contribute to higher bilirubin. Conversely, *Streptococcus thermophilus* and *Rothia* showed negative correlations with bilirubin levels (Fig. 2B–F). Correlation heatmap analysis confirmed these findings: the significantly increased genera *Streptococcus thermophilus* ($p < 0.001$) and *Rothia* ($p = 0.004$) were negatively correlated with total bilirubin, while the significantly decreased genera *Pseudomonas* ($p = 0.034$) and *Staphylococcus* ($p = 0.359$) were positively correlated. Additionally, *Bifidobacterium* ($p = 0.016$) was also negatively correlated with total bilirubin levels (Fig. 2G).

### *3.3 Differences in Fecal Metabolites Between the Pretherapy and Post-Treatment Groups*

Complementing the gut microbiota analysis, we performed LC-MS/MS to profile fecal metabolites in neonates with hyperbilirubinemia before and after treatment. Orthogonal partial least squares-discriminant analysis (OPLS-DA) revealed significant separation between pre- and post-treatment groups under both positive and negative ionization modes (Fig. 3A,B) (**Supplementary Material_plsda_score_neg/pos**). Differential analysis identified 25 significantly upregulated and 147 downregulated metabolites in positive ion mode, and 17 upregulated and 65 downregulated metabolites in negative ion mode post-treatment (Fig. 3C,D).

Correlations between significantly differential fecal metabolites and liver function indices pre- and post-treatment were analyzed. Metabolites meeting the criteria ($p < 0.05$ and correlation coefficient $>0.3$) were selected for inclusion in the correlation heatmap (Fig. 4A). We identified 15 fecal metabolites significantly correlated with total bilirubin levels. These included: Nine metabolites negatively correlated with total bilirubin, total protein, aspartate aminotransferase, and albumin levels: 9,10-DiHOME, DIPROTIN A, pyrophosphate, threonate, PE (18:1(9Z)/0:0), (+/-)8(9)-EET methyl ester, 9,11-methane-epoxy PGF1$\alpha$, and prostaglandin E2 isopropyl ester. Four metabolites positively correlated with total bilirubin, total protein, aspartate aminotransferase, and albumin levels: LS-Tetrasaccharide $\beta$, Putrescine, PC (18:3(6Z,9Z,12Z)/18:3(6Z,9Z,12Z)), and 3′-N-Acetylneuraminyl-N-acetyllactosamine. Two metabolites (Maltopentaose and Maltotetraose) showed a positive correlation with total bilirubin but a negative correlation with adenosine deaminase levels.

Furthermore, we investigated potential metabolic pathways of the differential fecal metabolites using KEGG pathway analysis. The enriched pathways predicted by KEGG indicated these metabolites were primarily associated with: biosynthesis of other secondary metabolites, metabolism of cofactors and vitamins, carbohydrate metabolism, xenobiotic biodegradation and metabolism, metabolism of other amino acids, energy metabolism, amino acid metabolism (Fig. 4B,C) (**Supplementary Material_KEGG_enrichment_result**).

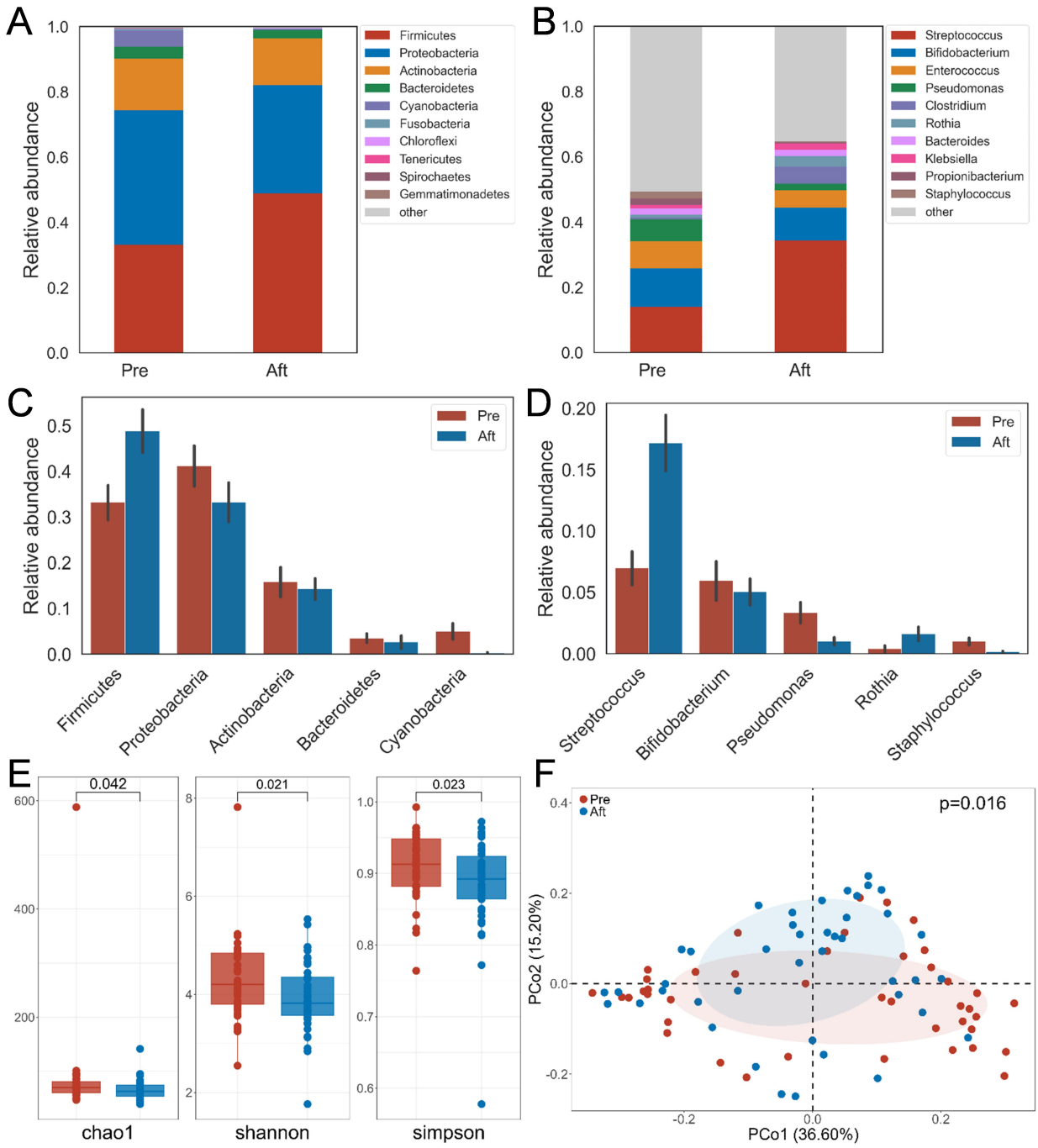


**Fig. 1. Gut microbiota alterations in neonates with hyperbilirubinemia pre- vs. post-treatment.** (A) Phylum-level composition. (B) Genus-level composition. (C) Top 5 phyla by relative abundance. (D) Top 5 genera by relative abundance. (E) Alpha diversity indices (Chao1, Shannon, Simpson). (F) Beta diversity (Principal Coordinate Analysis based on unweighted UniFrac distances).

### *3.4 Correlation Between the Differential Fecal Metabolites and Intestinal Microflora*

To investigate how gut microbiota structure influences the metabolic phenotype in hyperbilirubinemia, we analyzed correlations between differential bacterial genera and differential fecal metabolites pre- vs. post-treatment. Based on these correlations, we constructed a network diagram integrating gut microbiota, fecal metabolites, and liver function indices (Fig. 5A,B). Key findings include: *Pseudomonas*, which showed a positive correlation with total bilirubin, was also positively correlated with PC (18:3(6Z,9Z,12Z)/18:3(6Z,9Z,12Z)) and negatively correlated with (+/-)8(9)-EET methyl ester, 9,10-DiHOME, 9,11-methane-epoxy PGF1$\alpha$, DIPROTIN A, prostaglandin E2 isopropyl ester, and pyrophosphate. *Streptococcus thermophilus* and *Rothia*, both negatively correlated with total bilirubin, exhibited positive correlations with: (+/-)8(9)-EET methyl

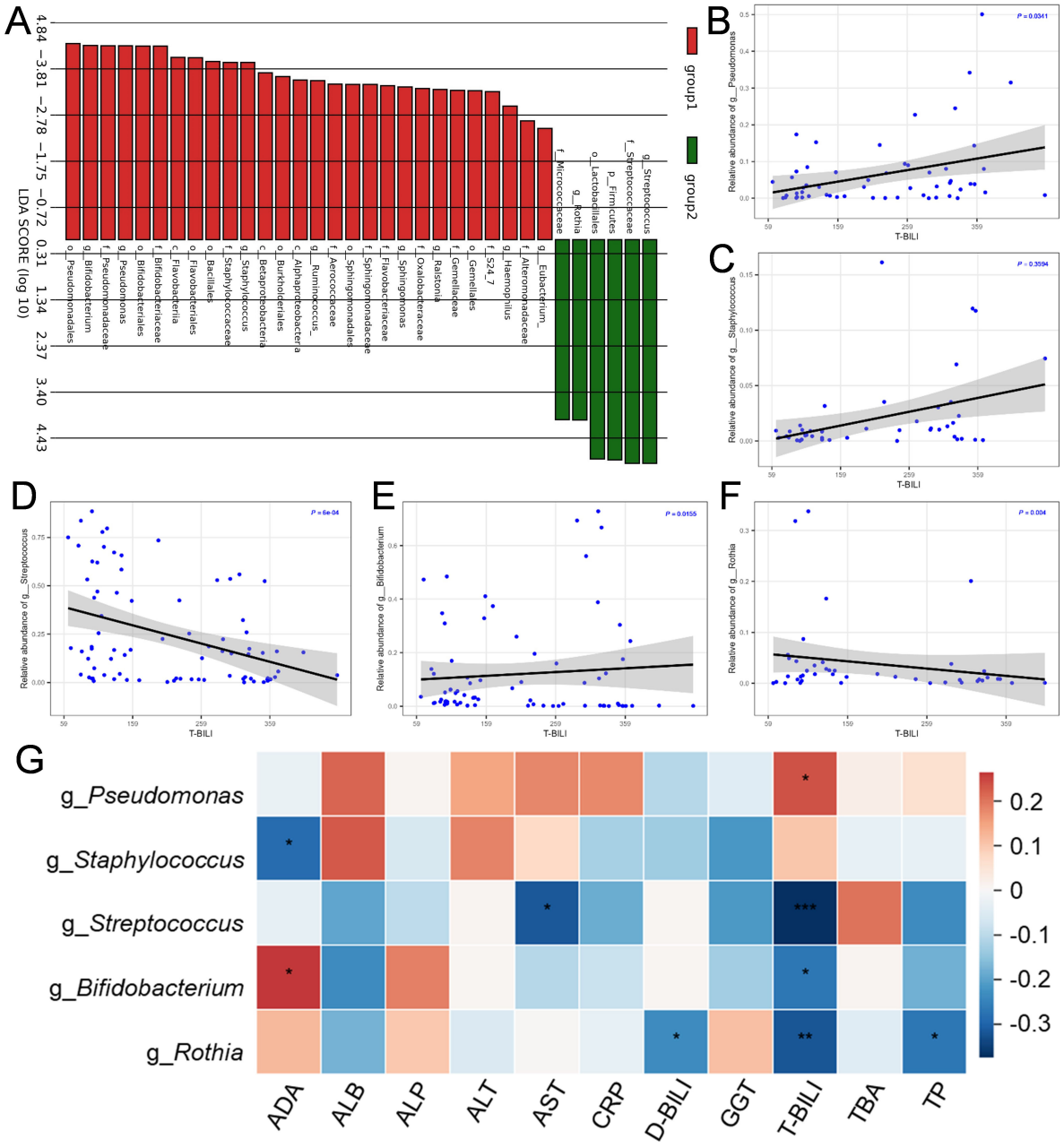


**Fig. 2. Gut microbiota alterations in neonates with hyperbilirubinemia pre- vs. post-treatment.** (A) Identification of differentially abundant taxa by LEfSe analysis (LDA score threshold $\geq$3.5). (B–F) Scatter plots with regression lines illustrating significant correlations between differentially abundant genera and total bilirubin levels. (G) Heatmap depicting Spearman's correlations between differentially abundant genera and liver function indices. *$p < 0.05$; **$p < 0.01$; ***$p < 0.001$.

ester, 9,11-methane-epoxy PGF1$\alpha$, DIPROTIN A, prostaglandin E2 isopropyl ester, and pyrophosphate and negative correlations with: 3′-N-acetylneuraminyl-N-acetyllactosamine, 7-methylthioheptyl glucosinolate, and PC (18:3(6Z,9Z,12Z)/18:3(6Z,9Z,12Z)).

## 4. Discussion

Neonatal jaundice, characterized by yellowish discoloration of the skin, mucous membranes, and sclera due to elevated serum bilirubin levels from impaired metabolism, is a common clinical condition broadly categorized as physiological or pathological. While physiological jaundice resolves spontaneously within days, severe pathological jaundice risks irreversible neurological damage, necessitating clinical vigilance [12].

The gut microbiota plays a crucial role in early bilirubin metabolism. As the body's most densely colonized site, the gut microbiota significantly influences host metabolism, immune function, and overall health [13,14]. In neonates, a healthy gut microbiota converts conjugated

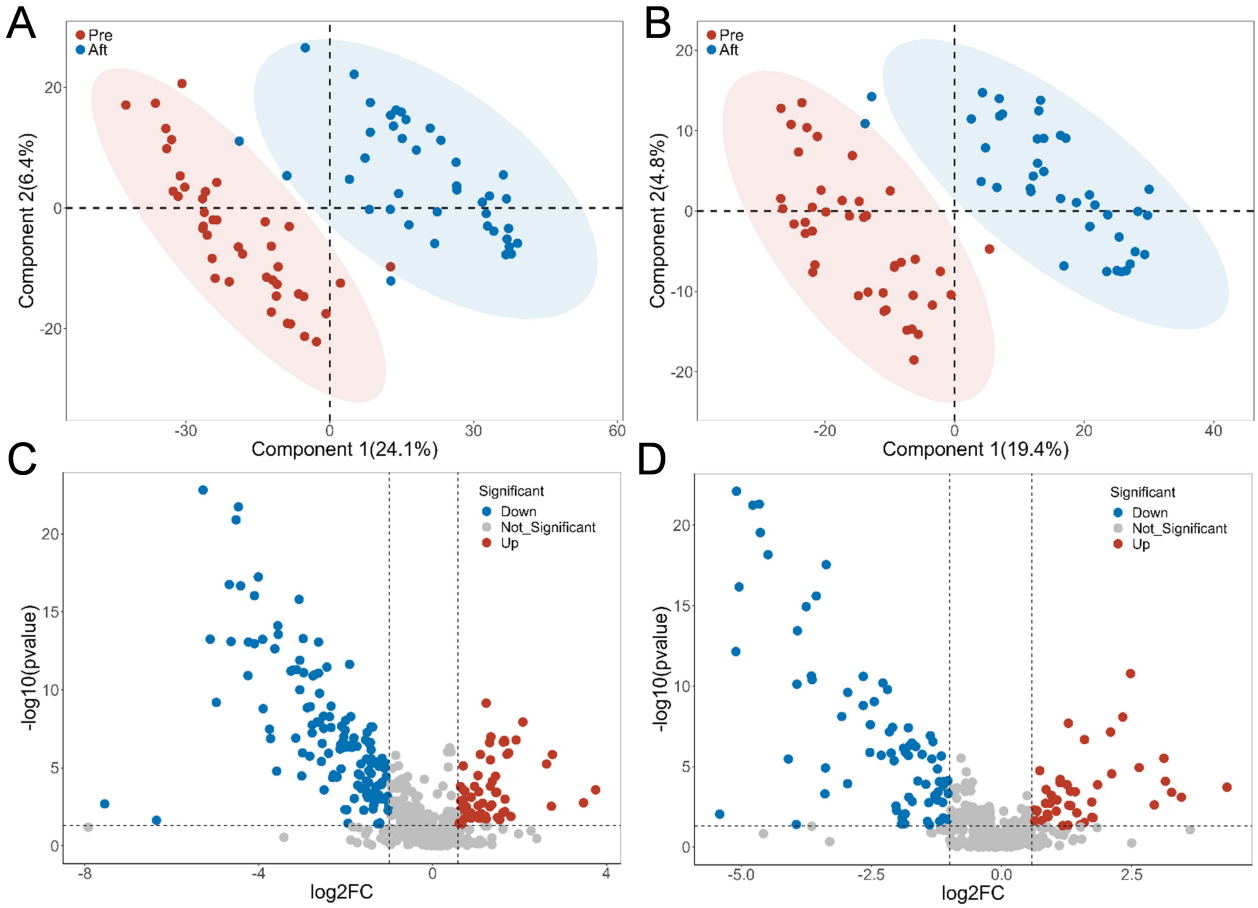


**Fig. 3. Fecal metabolome profile pre- vs. post-treatment.** (A,B) PLS-DA score plots of fecal metabolites in positive (A) and negative (B) ion modes. (C,D) Volcano plots of differential fecal metabolites in positive (C) and negative (D) ion modes.

bilirubin into fecal urobilinogen for excretion. However, intestinal immaturity can disrupt this balance, promoting bilirubin enterohepatic recirculation and contributing to hyperbilirubinemia. Altered microbial diversity, a hallmark of dysbiosis, is linked to various diseases, including metabolic disorders [15,16]. Our study observed significantly reduced gut microbial diversity post-treatment, corresponding with improved bilirubin metabolism. Beneficial bacteria like *Streptococcus thermophilus* and *Rothia* increased in abundance, while potentially detrimental bacteria decreased. Differential abundance of *Staphylococcus* and *Pseudomonas aeruginosa* pre- vs. post-treatment suggests their potential as hyperbilirubinemia biomarkers.

16S rRNA sequencing identified *Firmicutes*, *Proteobacteria*, *Actinobacteria*, *Bacteroidetes*, and *Cyanobacteria* as the dominant phyla in hyperbilirubinemic infants, consistent with early neonatal gut microbiota studies [17]. Post-treatment, *Firmicutes* abundance significantly increased while *Cyanobacteria* (pathogenic) decreased, aligning with Li *et al.*'s findings [18] of dysbiosis in hyperbilirubinemia. Neonatal gut colonization is complex: Proteobacteria (aerobic/facultative anaerobes) colonize first, followed by *Firmicutes* (anaerobes) as oxygen depletes. Diversity typically reaches near-adult levels within 7–10 days [19–21]. The pre-treatment *Firmicutes*-*Cyanobacteria* imbalance observed here suggests delayed colonization, potentially disrupting bilirubin metabolism [22,23].

In the metabolic process of bilirubin, unconjugated bilirubin primarily originates from heme. It binds to albumin in the blood and is transported to hepatocytes. In the liver, it is converted into conjugated bilirubin, which is then excreted into the intestine along with bile. Within the intestine, gut microbiota metabolize it into urobilinogen. A portion of the bilirubin derivatives is reabsorbed via the portal vein and returned to the liver. This process is known as the enterohepatic circulation of bilirubin [24]. It is well established that the gut-liver axis represents a bidirectional interaction system between the gut and the liver. They mutually influence each other through pathways including blood circulation, bile acids, and metabolic products. Dysbiosis of the gut microbiota may lead to metabolic imbalances, which can trigger metabolic abnormalities via the gut-liver axis and result in hyperbilirubinemia. However, to date, our

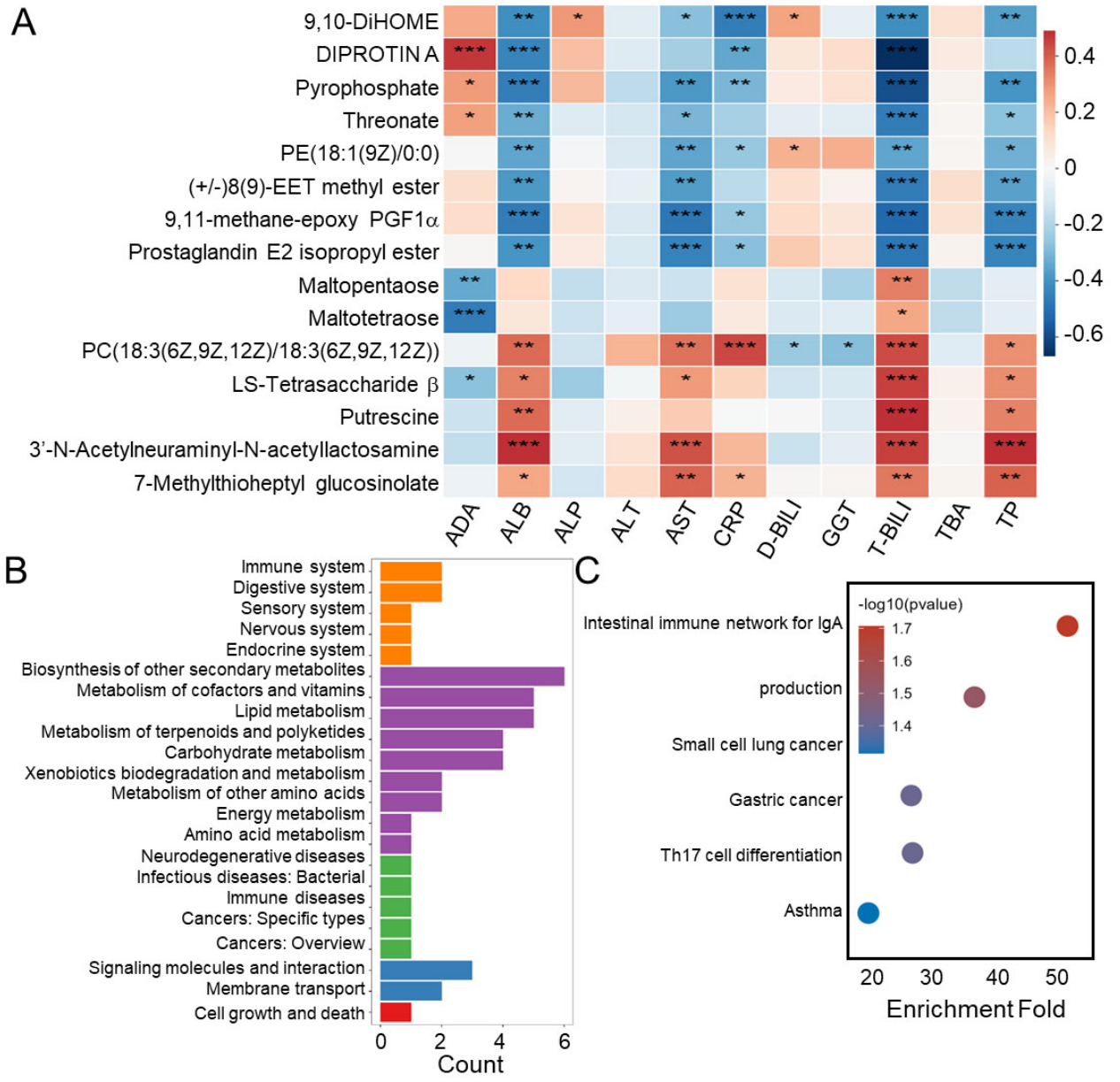


**Fig. 4. Correlation and pathway analysis of core differential metabolites.** (A) Heatmap showing Spearman correlations between liver function indices and core differential metabolites. Significance levels: *$p < 0.05$; **$p < 0.01$; ***$p < 0.001$. (B) KEGG pathway enrichment analysis of differential metabolites. (C) KEGG enrichment bubble chart displaying significant metabolic pathways.

understanding of the detailed pathways through which gut microbiota metabolize bilirubin remains limited [25].

At the genus level, *Rothia* and *Streptococcus thermophilus* abundance increased post-treatment, while *Pseudomonas* and *Staphylococcus* decreased. Probiotics combined with phototherapy likely promoted beneficial bacteria and suppressed pathogens. *Streptococcus thermophilus* inhibits pathogens and aids lactose digestion via $\beta$-galactosidase. *Rothia* promotes butyrate production, enhancing energy metabolism, short-chain fatty acid (SCFA) levels, gut barrier integrity, maturation, and bilirubin clearance [26]. Monitoring these genera could serve as biomarkers and therapeutic targets. Reduced *Staphylococcus* and *Pseudomonas* post-treatment suggests they may facilitate bilirubin enterohepatic recirculation, though mechanisms require elucidation [6]. This may be because elevated bilirubin within the physiological range exhibits toxic effects against Gram-positive bacteria (such as Staphylococcus aureus, Enterococcus faecalis, Bacillus cereus, and Streptococcus agalactiae), owing to their sensitivity to bilirubin. Bilirubin disrupts bacterial membranes, respiratory metabolism, and carbohydrate metabolism. Conversely, excessive bilirubin can promote the proliferation of Gram-positive staphylococci by neutralizing free radical attacks on the bacteria [27].

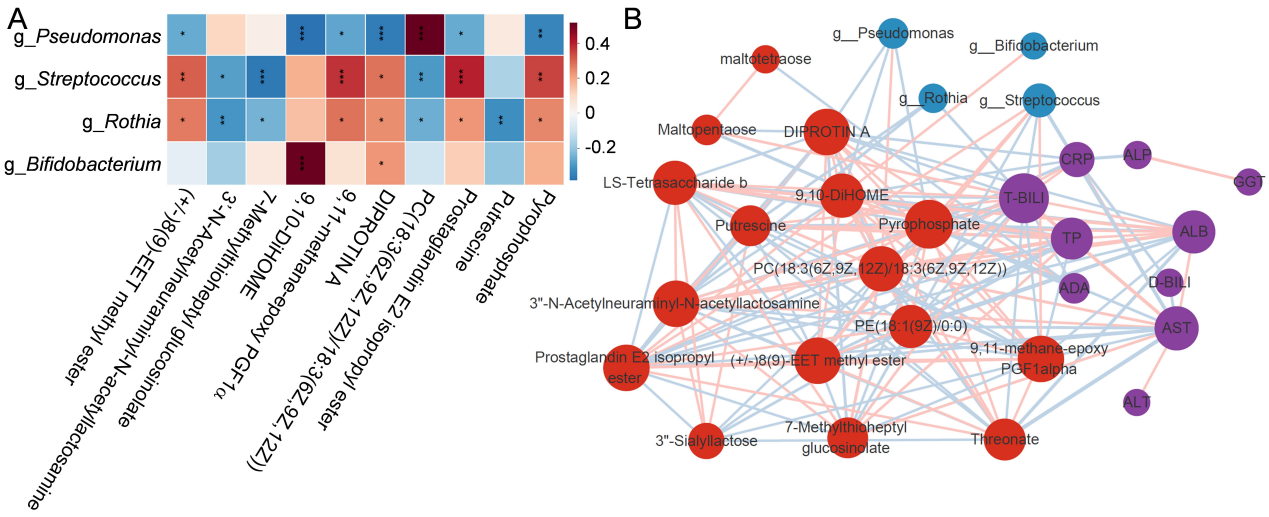


**Fig. 5. Correlation analysis between gut microbiota and core differential metabolites.** (A) Heatmap displaying Spearman correlations between core differential bacterial genera and fecal metabolites. Significance: $*p < 0.05$; $**p < 0.01$; $***p < 0.001$. (B) Correlation network integrating differential microbiota, fecal metabolites, and 10 liver function indices across pre- and post-treatment states.

Metabolomics reflects physiological status and reveals microbiota-host metabolic interactions [28,29]. Pathway analysis enriched differential metabolites in: secondary metabolite biosynthesis; cofactor/vitamin metabolism; carbohydrate metabolism; xenobiotic biodegradation/metabolism; energy metabolism; and amino acid metabolism. Spearman correlation revealed *Streptococcus thermophilus* and *Rothia* abundance positively correlated with (+/-)8(9)-EET methyl ester, 9,11-methane-epoxy PGF1$\alpha$, DIPROTIN A, prostaglandin E2 isopropyl ester, and pyrophosphate, and negatively correlated with 3′-N-Acetylneuraminyl-N-acetyllactosamine, 7-methylthioheptyl glucosinolate, and PC (18:3(6Z,9Z,12Z)/18:3(6Z,9Z,12Z)). *Streptococcus thermophilus* correlated most strongly with 9,11-methane-epoxy PGF1$\alpha$, prostaglandin E2 isopropyl ester, and 7-methylthioheptyl glucosinolate. Prostaglandin metabolites (9,11-methane-epoxy PGF1$\alpha$, prostaglandin E2 isopropyl ester) may protect liver function and promote repair via Akt pathway activation [30,31]. We hypothesize *S. thermophilus* modulates bilirubin metabolism by influencing prostaglandin metabolites and Akt signaling. Furthermore, *S. thermophilus* may convert inactive 7-methylthioheptyl glucosinolate into isothiocyanates [32], which exhibit anti-tumor, anti-inflammatory, and hepatoprotective effects via enzyme induction [33,34]. These metabolites potentially contribute to hyperbilirubinemia pathogenesis, warranting mechanistic investigation.

This study rigorously analyzed gut microbiota and fecal metabolite changes in 42 neonatal hyperbilirubinemia cases pre- and post-treatment. Limitations include unavoidable confounders (e.g., maternal diet, prenatal antibiotics) and the correlational nature of the data, which precludes establishing causality between gut microbiota and hyperbilirubinemia. Further research is needed to elucidate underlying mechanisms. Additionally, we used PASS software (Power Analysis and Sample Size, version 15.0) to calculate the power of this study, which was 76.6%, above 70%. Due to time and budget constraints, the sample size in this study was relatively small. This limitation suggests that the conclusions should be interpreted with caution. Including more participants could potentially enhance the reliability of the findings.

## 5. Conclusion

This study demonstrates significant alterations in gut microbiota composition and fecal metabolite profiles in neonates with hyperbilirubinemia following treatment. We observed reduced microbial diversity and resolved pre-treatment imbalances, particularly between *Firmicutes* and *Cyanobacteria*. Post-intervention, beneficial genera *Rothia* and *Streptococcus thermophilus* increased significantly, while *Pseudomonas* and *Staphylococcus* decreased substantially. Furthermore, fecal metabolites showed promise as diagnostic biomarkers for hyperbilirubinemia. These findings suggest that adjunctive gut microbiota modulation could enhance conventional neonatal hyperbilirubinemia therapies. This approach may enable microbiome-targeted interventions to improve clinical outcomes.

## Availability of Data and Materials

The datasets used and analyzed during the current study are available from the corresponding author on reasonable request.

## Author Contributions

CX, YL and DZL conceived and designed the research. LYW, YWL and CX performed the experiments. LYW, QQC and MXY analyzed the results and data. LYM and YWL wrote and YL revised the manuscript. All authors contributed to editorial changes in the manuscript. All authors read and approved the final manuscript. All authors have participated sufficiently in the work and agreed to be accountable for all aspects of the work.

## Ethics Approval and Consent to Participate

This study was approved by the ethics committee of The Fourth People's Hospital of Nanhai District of Foshan City (approved No. KKNL-2023-32). We certify that the study was performed in accordance with the 1964 declaration of HELSINKI and later amendments. Written informed consent to participate in this study was provided by the participants' legal guardian/next of kin.


## Acknowledgment

We thank the family members of all the included infants for their cooperation in this study. Also, we acknowledge Yilin Feng who earned her Master's degree from the University of Leicester (U.K.) for language polishing.

## Funding

This study was supported by the Scientific and technological innovation project of Foshan Science and technology development (2320001007307).


## Conflict of Interest

The authors declare no conflict of interest.

## Supplementary Material

Supplementary material associated with this article can be found, in the online version, at https://doi.org/10.31083/FBL42716.

## References


[1] Fouly AA, Bendas ER, Farid YA, Sabry S, Abou El Fadl DK. Different approaches in management of neonatal unconjugated hyperbilirubinemia: a review article. Future Journal of Pharmaceutical Sciences. 2024; 10: 171. https://doi.org/10.1186/s43094-024-00741-y.

[2] Chastain AP, Geary AL, Bogenschutz KM. Managing neonatal hyperbilirubinemia: An updated guideline. JAAPA: Official Journal of the American Academy of Physician Assistants. 2024; 37: 19–25. https://doi.org/10.1097/01.JAA.0000000000000120.

[3] Christensen RD, Bahr TM, Ohls RK, Moise KJ, Jr. Neonatal/perinatal diagnosis of hemolysis using ETCOc. Seminars in Fetal & Neonatal Medicine. 2025; 30: 101547. https://doi.org/10.1016/j.siny.2024.101547.

[4] Wismananda AV, Zahra AL, Lukinanda RK. Use of fenofibrate as adjuvant to phototherapy in unconjugated neonatal hyperbilirubinemia: A systematic review and meta-analysis of randomized controlled trials. Journal of Neonatal-perinatal Medicine. 2024; 17: 615–622. https://doi.org/10.3233/NPM-230189.

[5] Patel A, Vagha JD, Meshram RJ, Taksande A, Khandelwal R, Jain A, *et al*. Illuminating Progress: A Comprehensive Review of the Evolution of Phototherapy for Neonatal Hyperbilirubinemia. Cureus. 2024; 16: e55608. https://doi.org/10.7759/cureus.55608.

[6] Li J, Ye S, Huang X, Yang G, Wang Y, Zeng J, *et al*. Analysis of the intestinal microbiota and profiles of blood amino acids and acylcarnitines in neonates with hyperbilirubinemia. BMC Microbiology. 2024; 24: 171. https://doi.org/10.1186/s12866-024-03328-y.

[7] Wu R, Jiang Y, Yan J, Shen N, Liu S, Yin H, *et al*. Beneficial changes in gut microbiota after phototherapy for neonatal hyperbilirubinemia. Biomedical Reports. 2024; 20: 101. https://doi.org/10.3892/br.2024.1789.

[8] Preer GL, Philipp BL. Understanding and managing breast milk jaundice. Archives of Disease in Childhood. Fetal and Neonatal Edition. 2011; 96: F461–F466. https://doi.org/10.1136/adc.2010.184416.

[9] Koníčková R, Jirásková A, Zelenka J, Lešetický L, Štícha M, Vítek L. Reduction of bilirubin ditaurate by the intestinal bacterium Clostridium perfringens. Acta Biochimica Polonica. 2012; 59: 289–292.

[10] Silva YP, Bernardi A, Frozza RL. The Role of Short-Chain Fatty Acids From Gut Microbiota in Gut-Brain Communication. Frontiers in Endocrinology. 2020; 11: 25. https://doi.org/10.3389/fendo.2020.00025.

[11] Li YX, Zheng KD, Duan Y, Liu HJ, Tang YQ, Wu J, *et al*. Mass spectrometry-based identification of new serum biomarkers in patients with latent infection pulmonary tuberculosis. Medicine. 2022; 101: e32153. https://doi.org/10.1097/MD.0000000000032153.

[12] Wasser DE, Hershkovitz I. The question of ethnic variability and the Darwinian significance of physiological neonatal jaundice in East Asian populations. Medical Hypotheses. 2010; 75: 187–189. https://doi.org/10.1016/j.mehy.2010.02.017.

[13] Su H, Yang S, Chen S, Chen X, Guo M, Zhu L, *et al*. What Happens in the Gut during the Formation of Neonatal Jaundice-Underhand Manipulation of Gut Microbiota? International Journal of Molecular Sciences. 2024; 25: 8582. https://doi.org/10.3390/ijms25168582.

[14] Jiayi C, Jinying W, Yanhan Y, Tianyu L, Juanjuan C, Feng Z, *et al*. Probiotics' effects on gut microbiota in jaundiced neonates: a randomized controlled trial protocol. Frontiers in Pediatrics. 2024; 12: 1296517. https://doi.org/10.3389/fped.2024.1296517.

[15] You JJ, Qiu J, Li GN, Peng XM, Ma Y, Zhou CC, *et al*. The relationship between gut microbiota and neonatal pathologic jaundice: A pilot case-control study. Frontiers in Microbiology. 2023; 14: 1122172. https://doi.org/10.3389/fmicb.2023.1122172.

[16] Duan M, Han ZH, Huang T, Yang Y, Huang B. Characterization of gut microbiota and short-chain fatty acid in breastfed infants with or without breast milk jaundice. Letters in Applied Microbiology. 2021; 72: 60–67. https://doi.org/10.1111/lam.13382.

[17] Liou CS, Sirk SJ, Diaz CAC, Klein AP, Fischer CR, Higginbottom SK, *et al*. A Metabolic Pathway for Activation of Dietary Glucosinolates by a Human Gut Symbiont. Cell. 2020; 180: 717–728.e19. https://doi.org/10.1016/j.cell.2020.01.023.

[18] Li Y, Shen N, Li J, Hu R, Mo X, Xu L. Changes in Intestinal Flora and Metabolites in Neonates With Breast Milk Jaundice. Frontiers in Pediatrics. 2020; 8: 177. https://doi.org/10.3389/fped.2020.00177.

[19] Roswall J, Olsson LM, Kovatcheva-Datchary P, Nilsson S, Tremaroli V, Simon MC, *et al*. Developmental trajectory of the healthy human gut microbiota during the first 5 years of life.

Cell Host & Microbe. 2021; 29: 765–776.e3. https://doi.org/10.1016/j.chom.2021.02.021.
[20] Kundu P, Blacher E, Elinav E, Pettersson S. Our Gut Microbiome: The Evolving Inner Self. Cell. 2017; 171: 1481–1493. https://doi.org/10.1016/j.cell.2017.11.024.
[21] Hill CJ, Lynch DB, Murphy K, Ulaszewska M, Jeffery IB, O'Shea CA, *et al*. Evolution of gut microbiota composition from birth to 24 weeks in the INFANTMET Cohort. Microbiome. 2017; 5: 4. https://doi.org/10.1186/s40168-016-0213-y.
[22] Zhou S, Wang Z, He F, Qiu H, Wang Y, Wang H, *et al*. Association of serum bilirubin in newborns affected by jaundice with gut microbiota dysbiosis. The Journal of Nutritional Biochemistry. 2019; 63: 54–61. https://doi.org/10.1016/j.jnutbio.2018.09.016.
[23] Zhang X, Zeng S, Cheng G, He L, Chen M, Wang M, *et al*. Clinical Manifestations of Neonatal Hyperbilirubinemia Are Related to Alterations in the Gut Microbiota. Children (Basel, Switzerland). 2022; 9: 764. https://doi.org/10.3390/children9050764.
[24] Zhang Y, Luan H, Song P. Bilirubin metabolism and its application in disease prevention: mechanisms and research advances. Inflammation Research. 2025; 74: 81. https://doi.org/10.1007/s00011-025-02049-w.
[25] Albillos A, de Gottardi A, Rescigno M. The gut-liver axis in liver disease: Pathophysiological basis for therapy. Journal of Hepatology. 2020; 72: 558–577. https://doi.org/10.1016/j.jhep.2019.10.003.
[26] Liu XC, Du TT, Gao X, Zhao WJ, Wang ZL, He Y, *et al*. Gut microbiota and short-chain fatty acids may be new biomarkers for predicting neonatal necrotizing enterocolitis: A pilot study. Frontiers in Microbiology. 2022; 13: 969656. https://doi.org/10.3389/fmicb.2022.969656.
[27] Vítek L, Tiribelli C. Bilirubin: The yellow hormone? Journal of Hepatology. 2021; 75: 1485–1490. https://doi.org/10.1016/j.jhep.2021.06.010.
[28] Cao W, Liu Y, Zhang Z, Xu X. Lipid-lowering effects and metabolomic investigation of Polygonatum sibiricum fermented by Lactobacillus plantarum NX-1. Process Biochemistry. 2025; 153: 102–109. https://doi.org/10.1016/j.procbio.2025.03.007.
[29] Yu Y, Zhu J, Fu R, Guo L, Chen T, Xu Z, *et al*. Unique intestinal microflora and metabolic profile in different stages of hypertension reveal potential biomarkers for early diagnosis and prognosis. Journal of Medical Microbiology. 2024; 73. https://doi.org/10.1099/jmm.0.001839.
[30] Rudnick DA, Perlmutter DH, Muglia LJ. Prostaglandins are required for CREB activation and cellular proliferation during liver regeneration. Proceedings of the National Academy of Sciences of the United States of America. 2001; 98: 8885–8890. https://doi.org/10.1073/pnas.151217998.
[31] Yao L, Chen W, Han C, Wu T. Microsomal prostaglandin E synthase-1 protects against Fas-induced liver injury. American Journal of Physiology. Gastrointestinal and Liver Physiology. 2016; 310: G1071–G1080. https://doi.org/10.1152/ajpgi.00327.2015.
[32] Folkard DL, Melchini A, Traka MH, Al-Bakheit A, Saha S, Mulholland F, *et al*. Suppression of LPS-induced transcription and cytokine secretion by the dietary isothiocyanate sulforaphane. Molecular Nutrition & Food Research. 2014; 58: 2286–2296. https://doi.org/10.1002/mnfr.201400550.
[33] Shakour ZT, Shehab NG, Gomaa AS, Wessjohann LA, Farag MA. Metabolic and biotransformation effects on dietary glucosinolates, their bioavailability, catabolism and biological effects in different organisms. Biotechnology Advances. 2022; 54: 107784. https://doi.org/10.1016/j.biotechadv.2021.107784.
[34] Tian C, Deng S, Zhang Z, Zheng K, Wei L. Bifidobacterium bifidum 1007478 derived indole-3-lactic acid alleviates NASH via an aromatic hydrocarbon receptor-dependent pathway in zebrafish. Life Sciences. 2025; 369: 123557. https://doi.org/10.1016/j.lfs.2025.123557.